

Error Performance of MIMO-BICM with Zero-Forcing Receivers in Spatially-Correlated Rayleigh Channels

Matthew R. McKay, *Student Member, IEEE* and Iain B. Collings, *Senior Member, IEEE*

Abstract—In this letter we derive tight analytical expressions for the coded bit error rate of MIMO bit-interleaved coded modulation (BICM) in spatially-correlated Rayleigh fading channels. We consider the case where low complexity zero-forcing receivers are employed. The analysis is simpler and more direct than the standard BICM error event expurgation technique, and yields efficient, accurate expressions for the error probability. Based on the analytical results, we obtain the diversity order and show that it is independent of the spatial correlation. Moreover, we show that the presence of spatial correlation induces an SNR loss with respect to i.i.d. channels. We quantify this loss, and show that it is a function of the antenna configuration and the eigenvalues of the spatial correlation matrices, and is independent of the coding and modulation parameters.

Index Terms—BICM, MIMO, zero-forcing, spatial correlation

I. INTRODUCTION

Bit-interleaved coded modulation (BICM) is a pragmatic technique which can achieve large diversity orders in fading wireless channels [1]. Recently, BICM was employed in a multiple-input multiple-output (MIMO) antenna system with maximum likelihood (ML) detection [2], and was shown to outperform space-time trellis codes in fast fading conditions. Unfortunately, the computational complexity of the ML receiver increases exponentially with the product of the number of transmit antennas and the number of bits per modulation symbol, thereby making it prohibitive in practice. A reduced complexity scheme was proposed in [3], and analyzed in [4], which employed a linear zero-forcing (ZF) receiver. It was shown in [4] that this receiver has desirable signal-space properties in i.i.d. Rayleigh fading MIMO-BICM systems, which allow near-ML performance to be achieved in many scenarios. The challenge is to investigate the performance of this practical low-complexity receiver in the more common case of spatially-correlated channels.

In this letter, we derive tight analytical expressions for the coded bit error rate (BER) of MIMO-BICM with ZF receivers

Manuscript received April 13, 2005; revised October 14, 2005; accepted November 4, 2005. The editor coordinating the review of this paper and approving it for publication is J. Garcia-Frias. This paper was presented in part at the Australian Communication Theory Workshop (AusCTW), Perth, Australia, Feb. 2006.

M. R. McKay is with the Telecommunications Laboratory, School of Electrical and Information Engineering, University of Sydney, NSW, Australia, and also the Wireless Technologies Laboratory, ICT Centre, CSIRO, Australia. I. B. Collings is with the Wireless Technologies Laboratory, ICT Centre, CSIRO, Australia. (e-mail: mckay@ee.usyd.edu.au; Iain.Collings@csiro.au).

Digital Object Identifier: 00.0000/TWC.2005.000000

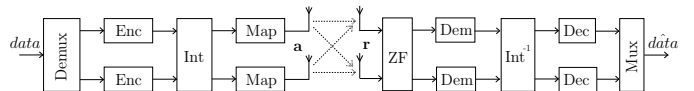


Fig. 1. Structure of a MIMO-BICM system with a zero-forcing receiver and 2×2 antennas.

(hereafter denoted ZF-BICM) in spatially-correlated channels. The results are for Gray-labeled PSK/QAM constellations¹, and are based on the typical BICM assumption of ideal interleaving. Our analysis is simpler and more direct than the standard BICM expurgation technique (eg. as used in [1, 4]), and yields accurate, efficient BER expressions for channels with transmit and receive spatial correlation. Based on the analytical results, we obtain the diversity order and show that it is independent of the spatial correlation. Moreover, we show that the presence of spatial correlation induces an SNR loss with respect to i.i.d. channels. We quantify this loss, and show that it is a function of the antenna configuration and the eigenvalues of the spatial correlation matrices, and is independent of the coding and modulation parameters.

II. SIGNAL MODEL

Consider a MIMO-BICM system with N_t transmit and N_r receive antennas (denoted $N_t \times N_r$). Fig. 1 shows the transmitter structure with separate modulators/encoders applied on each of the transmit layers. The data sequence is cyclically demultiplexed across the layers and each resulting stream is binary convolutionally encoded. Bit interleaving is applied within and across the layers, prior to mapping to Gray-labelled 2^M -ary QAM or PSK for transmission.

The received signal vector is given by

$$\mathbf{r} = \sqrt{\gamma} \mathbf{H} \mathbf{a} + \mathbf{n} \quad (1)$$

where $\mathbf{a} \in \mathcal{C}^{N_t \times 1}$ is the transmitted vector with i^{th} element a_i chosen from the complex scalar constellation \mathcal{A} with unit average power, $\mathbf{n} \in \mathcal{C}^{N_r \times 1}$ is the noise vector $\sim \mathcal{CN}(\mathbf{0}_{N_r \times 1}, \mathbf{I}_{N_r})$, and γ is the average SNR per transmit antenna. Also, $\mathbf{H} \in \mathcal{C}^{N_r \times N_t}$ is the spatially-correlated channel matrix, assumed to be known perfectly at the receiver, having the (common) correlation structure

$$\mathbf{H} = \mathbf{R}^{\frac{1}{2}} \mathbf{H}_w \mathbf{S}^{\frac{1}{2}} \quad (2)$$

¹We note that the analysis approach could be extended to other labelings, but is beyond the scope of this letter.

where $\mathbf{R} \in \mathcal{C}^{N_r \times N_r}$ and $\mathbf{S} \in \mathcal{C}^{N_t \times N_t}$ are the normalized receive and transmit correlation matrices respectively, and $\mathbf{H}_w \in \mathcal{C}^{N_r \times N_t}$ contains independent entries $H_{i,j} \sim \mathcal{CN}(0, 1)$. As such, the average SNR per receive antenna is $N_t \gamma$.

At the receiver, the ZF filtering step is

$$\begin{aligned} \mathbf{z} &= \mathbf{W} \mathbf{r} \\ &= \sqrt{\gamma} \mathbf{a} + \mathbf{n} \end{aligned} \quad (3)$$

where $\mathbf{W} = (\mathbf{H}^\dagger \mathbf{H})^{-1} \mathbf{H}^\dagger$ and $\mathbf{n} = \mathbf{W} \mathbf{n}$. The BICM log-likelihood metrics for each of the bits i ($= 1, \dots, M$) corresponding to a_k are calculated from z_k using

$$\begin{aligned} \mathcal{L}_{k,i} &= \ln \frac{\sum_{\tilde{a}_k \in \mathcal{A}_1^{i,k}} p(z_k | \tilde{a}_k, \mathbf{w}_k)}{\sum_{\tilde{a}_k \in \mathcal{A}_0^{i,k}} p(z_k | \tilde{a}_k, \mathbf{w}_k)} \\ &= \ln \frac{\sum_{\tilde{a}_k \in \mathcal{A}_1^{i,k}} \exp\left(-\frac{|z_k - \sqrt{\gamma} \tilde{a}_k|^2}{\|\mathbf{w}_k\|^2}\right)}{\sum_{\tilde{a}_k \in \mathcal{A}_0^{i,k}} \exp\left(-\frac{|z_k - \sqrt{\gamma} \tilde{a}_k|^2}{\|\mathbf{w}_k\|^2}\right)} \end{aligned} \quad (4)$$

where $\mathcal{A}_0^{i,k}, \mathcal{A}_1^{i,k}$ are the signal subsets within the k^{th} transmit constellation with i^{th} bit equal to 0 and 1 respectively. These metrics are deinterleaved into the appropriate output streams, and each parallel stream is decoded using a conventional soft-decision Viterbi algorithm.

III. ERROR PERFORMANCE ANALYSIS IN SPATIALLY-CORRELATED MIMO CHANNELS

A. BER Union Bound

Throughout this paper we consider linear binary convolutional codes with rate $R_c = k_c/n_c$, for which a tight BER union bound is given by [5]

$$P_b \leq \frac{1}{k_c} \sum_{d=d_{\text{free}}}^{\infty} W_I(d) f(d, \mu, \mathcal{A}, \gamma) \quad (5)$$

where $W_I(d)$ is the input weight of all error events at Hamming distance d , and $f(\cdot)$ is the codeword pairwise error probability (C-PEP) which is also a function of the labeling map μ , the signal set \mathcal{A} , and the SNR γ . Also, d_{free} is the free Hamming distance.

B. Evaluation of the C-PEP

For the ZF-BICM system operating under the assumption of ideal interleaving, the BICM metrics which are fed into the decoder for each stream are i.i.d. Consequently, each encoder-decoder pair acts as an equivalent single-input single-output (SISO) BICM system with the same error characteristics; thereby allowing us to focus on a single arbitrary stream error probability. We also adopt the approach of [1] and force the BICM subchannels² to behave as binary-input output-symmetric (BIOS) channels by introducing a time-varying labeling map. Specifically, we define u as a random variable which independently selects, for every MIMO transmission, the labeling map μ or its complement $\bar{\mu}$ with probability $\frac{1}{2}$ ³.

²These are the equivalent channels between the transmitted binary codeword and the corresponding BICM bit metrics.

³Note that in the following we select $\bar{\mu}$ when $u = 1$.

Further assuming that the all-zero codeword is transmitted, we have the following well-known result for BIOS channels [5]

$$f(d, \mu, \mathcal{A}, \gamma) = \Pr\left(\sum_{i=1}^d \mathcal{L}_i > 0\right) \quad (6)$$

where, in this ZF-BICM case

$$\mathcal{L}_i = \ln \frac{\sum_{\tilde{a} \in \mathcal{A}_{\tilde{a}_i}^{m_i, k}} \exp\left(-\frac{|z_i - \sqrt{\gamma} \tilde{a}|^2}{\|\mathbf{w}_{i,k}\|^2}\right)}{\sum_{\tilde{a} \in \mathcal{A}_u^{m_i, k}} \exp\left(-\frac{|z_i - \sqrt{\gamma} \tilde{a}|^2}{\|\mathbf{w}_{i,k}\|^2}\right)} \quad (7)$$

where m_i is the bit position in the transmitted symbol's binary label which corresponds to the i^{th} equivalent binary-input transmission. Unfortunately \mathcal{L}_i is a complicated function for which the distribution (and hence the tail probability in (6)) is difficult to calculate. We can however evaluate the tail probability based on the moment generating function (m.g.f.) $\mathcal{M}(\cdot)$ as [6]

$$f(d, \mu, \mathcal{A}, \gamma) = \frac{1}{2\pi j} \int_{c-j\infty}^{c+j\infty} \mathcal{M}_{\sum_{i=1}^d \mathcal{L}_i}(s) \frac{ds}{s} \quad (8)$$

Since the likelihood ratios are i.i.d. under the assumption of ideal interleaving, we have⁴

$$f(d, \mu, \mathcal{A}, \gamma) = \frac{1}{2\pi j} \int_{c-j\infty}^{c+j\infty} \mathcal{M}_{\mathcal{L}}(s)^d \frac{ds}{s} \quad (9)$$

where

$$\begin{aligned} \mathcal{M}_{\mathcal{L}}(s) &= E_{Z, m, u, k, \mathbf{w}_k} \left[\exp\left(s \ln \frac{\sum_{\tilde{a} \in \mathcal{A}_u^{m, k}} \exp\left(-\frac{|z - \sqrt{\gamma} \tilde{a}|^2}{\|\mathbf{w}_k\|^2}\right)}{\sum_{\tilde{a} \in \mathcal{A}_u^{m, k}} \exp\left(-\frac{|z - \sqrt{\gamma} \tilde{a}|^2}{\|\mathbf{w}_k\|^2}\right)}\right)\right] \\ &= E_{a, m, u, k, \mathbf{w}_k} \left[\left(\frac{\sum_{\tilde{a} \in \mathcal{A}_u^{m, k}} \exp\left(-\frac{|\sqrt{\gamma}(a - \tilde{a}) + \mathbf{n}_k|^2}{\|\mathbf{w}_k\|^2}\right)}{\sum_{\tilde{a} \in \mathcal{A}_u^{m, k}} \exp\left(-\frac{|\sqrt{\gamma}(a - \tilde{a}) + \mathbf{n}_k|^2}{\|\mathbf{w}_k\|^2}\right)} \right)^s \right] \end{aligned} \quad (10)$$

Averaging over m, u, k and $a \in \mathcal{A}_u^{m, k}$ gives

$$\mathcal{M}_{\mathcal{L}}(s) = \frac{1}{M 2^M N_t} \sum_{m=1}^M \sum_{u=0}^1 \sum_{k=1}^{N_t} \sum_{a \in \mathcal{A}_u^{m, k}} \mathcal{I}_{m, u, a}(s) \quad (11)$$

where

$$\begin{aligned} \mathcal{I}_{m, u, k, a}(s) &= \\ &= E_{\mathbf{w}_k, \mathbf{w}_k} \left[\left(\frac{\sum_{\tilde{a} \in \mathcal{A}_u^{m, k}} \exp\left(-\frac{|\sqrt{\gamma}(a - \tilde{a}) + \mathbf{n}_k|^2}{\|\mathbf{w}_k\|^2}\right)}{\sum_{\tilde{a} \in \mathcal{A}_u^{m, k}} \exp\left(-\frac{|\sqrt{\gamma}(a - \tilde{a}) + \mathbf{n}_k|^2}{\|\mathbf{w}_k\|^2}\right)} \right)^s \right] \end{aligned} \quad (12)$$

We note that the expectation (12) can be evaluated via numerical integration using a combination of Gauss-Laguerre and Gauss-Hermite quadratures [7], and the integral in (9) evaluated using Gauss-Chebyshev quadratures [8].

We now show that at high SNR, computing $f(\cdot)$ reduces to only a single numerical integration - the result of which can be written in closed form. Note that at high SNR the ratio in (12) is dominated by a single (minimum distance)

⁴Note that we drop the subscript on \mathcal{L} when we are considering the log likelihood ratio statistics at a single instant in time.

$$\Psi_t = \left(\frac{1}{N_t} \sum_{k=1}^{N_t} \sum_{i=1}^{|\mathcal{P}_M|} \mathcal{P}_{M,i} \frac{\text{tr}_{N_t-1}(\lambda(\mathbf{R})) \det \left(\mathbf{I}_{N_r} + \frac{\gamma \mathcal{E}_{M,i} (1 + \tan^2(\frac{(2t-1)\pi}{2v})) \lambda(\mathbf{R})}{4[\mathbf{S}^{-1}]_{k,k}} \right)^{-1}}{\text{tr}_{N_t-1} \left(\lambda(\mathbf{R}) \left[\mathbf{I}_{N_r} + \frac{\gamma \mathcal{E}_{M,i} (1 + \tan^2(\frac{(2t-1)\pi}{2v})) \lambda(\mathbf{R})}{4[\mathbf{S}^{-1}]_{k,k}} \right]^{-1} \right)} \right)^d \quad (20)$$

term in the numerator and denominator, and as such we can apply the Dominated Convergence Theorem [9]. (The Dominated Convergence Theorem has previously been used in the analysis of BICM [10, App. III] where they considered SISO systems and were deriving the asymptotic slope of the error probability.) We now have

$$\mathcal{I}_{m,u,k,a}(s) = E_{\underline{n}_k, \mathbf{w}_k} \left[\left(\frac{\exp \left(-\frac{|\sqrt{\gamma}(a-\tilde{a}) + \underline{n}_k|^2}{\|\mathbf{w}_k\|^2} \right)}{\exp \left(-\frac{|\underline{n}_k|^2}{\|\mathbf{w}_k\|^2} \right)} \right)^s \right] \quad (13)$$

where $\tilde{a} \in \mathcal{A}_u^{m,k}$ is the nearest neighbour to $a \in \mathcal{A}_u^{m,k}$. We proceed to average over the random noise as follows

$$\begin{aligned} \mathcal{I}_{m,u,k,a}(s) &= E_{\mathbf{w}_k, \underline{n}_k} \left[\exp \left(\frac{-s|\sqrt{\gamma}(a-\tilde{a}) + \underline{n}_k|^2 + s|\underline{n}_k|^2}{\|\mathbf{w}_k\|^2} \right) \right] \\ &= E_{\mathbf{w}_k, \underline{n}_k} \left[\exp \left(\frac{-s\gamma|a-\tilde{a}|^2 - 2s\text{Re}(\sqrt{\gamma}(a-\tilde{a})\underline{n}_k^*)}{\|\mathbf{w}_k\|^2} \right) \right] \\ &= E_{\mathbf{w}_k} \left[\exp \left(\frac{-s\gamma|a-\tilde{a}|^2}{\|\mathbf{w}_k\|^2} \right) \int \frac{1}{\pi} \exp \left(\frac{s^2\gamma|a-\tilde{a}|^2}{\|\mathbf{w}_k\|^2} \right) \right. \\ &\quad \left. \times \exp \left(\frac{-|\underline{n}_k + s\sqrt{\gamma}(a-\tilde{a})|^2}{\|\mathbf{w}_k\|^2} \right) d\underline{n}_k \right] \\ &= E_{\mathbf{w}_k} \left[\exp \left(\frac{-\gamma|a-\tilde{a}|^2 s(1-s)}{\|\mathbf{w}_k\|^2} \right) \right]. \end{aligned} \quad (14)$$

It is now possible to express the expectation (14) in the form of an integral equation, however it appears difficult to evaluate the resulting expression in closed form. However, we can obtain a simple and accurate closed-form approximation by first noting that (14) can be written as

$$\mathcal{I}_{m,u,k,a}(s) = \mathcal{M}_{\gamma/\|\mathbf{w}_k\|^2}(-|a-\tilde{a}|^2 s(1-s)). \quad (15)$$

Using the Laplace approximation to the ratio of quadratic forms [11], a general expression for the m.g.f. $\mathcal{M}_{\gamma/\|\mathbf{w}_k\|^2}(\cdot)$ was first obtained in [12], which considered the analysis of symbol error probabilities in uncoded ZF systems. Applying this result in (15), we have

$$\begin{aligned} \mathcal{I}_{m,u,k,a}(s) &\approx \det \left(\mathbf{I}_{N_r} + \frac{\gamma|a-\tilde{a}|^2 s(1-s)\lambda(\mathbf{R})}{[\mathbf{S}^{-1}]_{k,k}} \right)^{-1} \\ &\quad \times \frac{\text{tr}_{N_t-1}(\lambda(\mathbf{R}))}{\text{tr}_{N_t-1} \left(\lambda(\mathbf{R}) \left[\mathbf{I}_{N_r} + \frac{\gamma|a-\tilde{a}|^2 s(1-s)\lambda(\mathbf{R})}{[\mathbf{S}^{-1}]_{k,k}} \right]^{-1} \right)} \end{aligned} \quad (16)$$

where $\lambda(\cdot)$ denotes a diagonal matrix containing the eigenvalues of the matrix argument, and $[\cdot]_{k,k}$ represents the k^{th} diagonal element. Also, $\text{tr}_\ell(\cdot)$ denotes the ℓ^{th} elementary symmetric function (e.s.f.) defined as [13, 14]

$$\text{tr}_\ell(\mathbf{X}) = \sum_{\{\alpha\}} \prod_{i=1}^{\ell} \lambda_{x,\alpha_i} = \sum_{\{\alpha\}} \det \left(\mathbf{X}_{\alpha}^{\alpha} \right) \quad (17)$$

for arbitrary Hermitian positive-definite $\mathbf{X} \in \mathcal{C}^{n \times n}$, where the sum is over all ordered $\alpha = \{\alpha_1, \dots, \alpha_\ell\} \subseteq \{1, \dots, n\}$, $\lambda_{x,i}$ denotes the i^{th} eigenvalue of \mathbf{X} , and $\mathbf{X}_{\alpha}^{\alpha}$ is an $\ell \times \ell$ matrix formed by taking only the rows and columns indexed by α .

Now, substituting (16) into (11) gives a closed-form expression for the m.g.f. Unfortunately this is quite numerically challenging to evaluate, since it requires calculation of $M2^M N_t$ terms $\mathcal{I}_{m,u,a}(s)$, each containing determinants and e.s.f.s. We can see from (16) however, that $\mathcal{I}_{m,u,a}(s)$ only depends on a through the squared Euclidean distance to its nearest neighbour \tilde{a} in the complement subset. Since in this paper we consider Gray-labelled PSK/QAM constellations, we can further simplify (11) by exploiting multiplicities of the Euclidean distances. In Table I we present (for BPSK, QPSK, 16QAM, and 64QAM Gray-labelled constellations) the set of all distinct squared Euclidean distances \mathcal{E}_M , and the corresponding set \mathcal{P}_M containing the frequency of occurrence of each distance (this is the number of occurrences of each distance in the summations over m, u and a in (11), normalized by the total number of distances, $M2^M$).

	\mathcal{P}_M	\mathcal{E}_M
BPSK	{1}	{4.0}
QPSK	{1}	{2.0}
16QAM	{3/4, 1/4}	{0.4, 1.6}
64QAM	{7/12, 1/4, 1/12, 1/12}	{0.0952, 0.3810, 0.8571, 1.5238}

TABLE I
BREAKDOWN OF DISTANCE MULTIPLICITIES BETWEEN COMPLEMENT BICM SUBSETS FOR VARIOUS GRAY-LABELLED CONSTELLATIONS

	All Distances	Simplified
BPSK	4	2
QPSK	16	2
16QAM	128	4
64QAM	768	8

TABLE II
COMPARISON BETWEEN NUMBER OF TERMS IN THE C-PEP EXPRESSION, BEFORE AND AFTER SIMPLIFICATION USING DISTANCE MULTIPLICITIES.

In this way, the m.g.f. (11) can be written as

$$\mathcal{M}_{\mathcal{L}}(s) = \frac{1}{N_t} \sum_{k=1}^{N_t} \sum_{i=1}^{|\mathcal{P}_M|} \mathcal{P}_{M,i} \tilde{\mathcal{I}}_{k,\mathcal{E}_{M,i}}(s) \quad (18)$$

where $|\cdot|$ represents set cardinality, $\mathcal{P}_{M,i}$ and $\mathcal{E}_{M,i}$ denote the i^{th} element of \mathcal{P}_M and \mathcal{E}_M respectively, and $\tilde{\mathcal{I}}_{k,\mathcal{E}_{M,i}}(s)$ is given as in (16), but with the factor $|a - \tilde{a}|^2$ replaced by $\mathcal{E}_{M,i}$. In Table II we compare the number of terms in (18) and (11) for $N_t = 2$, and for various modulation schemes. We see that (18) yields a significant computational advantage over (11), especially for high order constellations.

We finally substitute (18) into (9), apply the Gauss-Chebyshev quadrature rules to the single remaining integration, and simplify to obtain

$$f(d, \mu, \mathcal{A}, \gamma) \approx \frac{1}{v} \sum_{t=1}^{\frac{v}{2}} \left(\Re[\Psi_t] + \tan\left(\frac{(2t-1)\pi}{2v}\right) \Im[\Psi_t] \right) \quad (19)$$

where Ψ_t is given by (20) at the top of the page. Note that, in using Gauss-Chebyshev quadratures to evaluate the integral (9), we have selected $c = \hat{s}$, where \hat{s} is the *saddlepoint*, which corresponds to the real value of s which minimizes $\mathcal{M}_{\mathcal{L}}(s)$. It is easily verified that $\hat{s} = \frac{1}{2}$. Also note that the parameter v in (19) is chosen for convergence. We find that $v = 16$ is sufficient for all cases considered in this paper.

C. Chernoff Bound on the C-PEP

We now present a closed-form bound on the C-PEP (6). Since the C-PEP is the tail probability of a sum of i.i.d. random variables, we apply the Chernoff bound [15] which gives

$$\begin{aligned} f(d, \mu, \mathcal{A}, \gamma) &\leq f_{\text{ch}}(d, \mu, \mathcal{A}, \gamma) \\ &= \mathcal{M}_{\mathcal{L}}(\hat{s})^d. \end{aligned} \quad (21)$$

Using (18) and (16) (with appropriate modifications for $\tilde{\mathcal{I}}_{k,\mathcal{E}_{M,i}}(\cdot)$) we obtain

$$f_{\text{ch}}(d, \mu, \mathcal{A}, \gamma) = \left(\frac{1}{N_t} \sum_{k=1}^{N_t} \sum_{i=1}^{|\mathcal{P}_M|} \mathcal{P}_{M,i} \frac{\text{tr}_{N_t-1}(\lambda(\mathbf{R})) \det\left(\mathbf{I}_{N_r} + \frac{\gamma \mathcal{E}_{M,i} \lambda(\mathbf{R})}{4[\mathbf{S}^{-1}]_{k,k}}\right)^{-1}}{\text{tr}_{N_t-1}\left(\lambda(\mathbf{R}) \left[\mathbf{I}_{N_r} + \frac{\gamma \mathcal{E}_{M,i} \lambda(\mathbf{R})}{4[\mathbf{S}^{-1}]_{k,k}}\right]^{-1}\right)} \right)^d \quad (22)$$

For high SNR, we neglect the identity terms in (22), and simplify the numerator as follows

$$\det\left(\frac{\gamma \mathcal{E}_{M,i} \lambda(\mathbf{R})}{4[\mathbf{S}^{-1}]_{k,k}}\right)^{-1} = \left(\frac{\gamma \mathcal{E}_{M,i}}{4[\mathbf{S}^{-1}]_{k,k}}\right)^{-N_r} \det(\mathbf{R})^{-1} \quad (23)$$

and the denominator, using the definition (17), to give

$$\begin{aligned} \text{tr}_{N_t-1}\left(\lambda(\mathbf{R}) \left[\frac{\gamma \mathcal{E}_{M,i} \lambda(\mathbf{R})}{4[\mathbf{S}^{-1}]_{k,k}}\right]^{-1}\right) &= \\ &= \left(\frac{\gamma \mathcal{E}_{M,i}}{4[\mathbf{S}^{-1}]_{k,k}}\right)^{1-N_t} \binom{N_r}{N_t-1}. \end{aligned} \quad (24)$$

Also, we can make use of the property [14]

$$[\mathbf{S}^{-1}]_{k,k} = \frac{\det(\mathbf{S}^{kk})}{\det(\mathbf{S})} \quad (25)$$

where \mathbf{S}^{kk} corresponds to \mathbf{S} with the k^{th} row and column removed. Combining (22)-(25) gives

$$f_{\text{ch}}(d, \mu, \mathcal{A}, \gamma) = \left(\frac{\gamma K_S K_R}{4}\right)^{-d(N_r - N_t + 1)} \quad (26)$$

where K_R and K_S are correlation factors corresponding to the receive and transmit correlation matrices respectively, given by

$$\begin{aligned} K_R &\triangleq \left(\frac{\text{tr}_{N_t-1}(\lambda(\mathbf{R}))}{\binom{N_r}{N_t-1} \det(\mathbf{R})}\right)^{-\frac{1}{N_r - N_t + 1}} \\ K_S &\triangleq \left(\frac{\det(\mathbf{S})^{-(N_r - N_t + 1)}}{N_t} \sum_{k=1}^{N_t} \sum_{i=1}^{|\mathcal{P}_M|} \mathcal{P}_{M,i} \right. \\ &\quad \left. \times \left(\frac{\mathcal{E}_{M,i}}{\det(\mathbf{S}^{kk})}\right)^{-(N_r - N_t + 1)}\right)^{-\frac{1}{N_r - N_t + 1}}. \end{aligned} \quad (27)$$

To obtain the diversity order, we substitute (26) into (5) and simplify by noting that error sequences with minimum Hamming weight d_{free} dominate in the high SNR regime, to obtain

$$\begin{aligned} \log_{10} P_b &\approx -d_{\text{free}}(N_r - N_t + 1) \\ &\quad \times \left[\gamma_{\text{dB}} + (K_R)_{\text{dB}} + (K_S)_{\text{dB}} + \left(\frac{W_I(d_{\text{free}})}{4k_c}\right)_{\text{dB}} \right] / 10 \end{aligned} \quad (28)$$

where $(\cdot)_{\text{dB}}$ is shorthand for $10 \log_{10}(\cdot)$. We clearly see that ZF-BICM achieves the diversity order $d_{\text{free}}(N_r - N_t + 1)$ in spatially-correlated Rayleigh MIMO channels.

D. Effect of Spatial Correlation at High SNR

In this subsection we examine more closely the effect of spatial correlation on the BER performance of ZF-BICM at high SNR. As a reference, we consider the Chernoff bound result (28) in the i.i.d. Rayleigh case, which is easily evaluated by setting $\mathbf{S} = \mathbf{I}_{N_t}$ and $\mathbf{R} = \mathbf{I}_{N_r}$ as⁵

$$\begin{aligned} \log_{10} \tilde{P}_b &\approx -d_{\text{free}}(N_r - N_t + 1) \\ &\quad \times \left[\gamma_{\text{dB}} + \left(\left(\sum_{i=1}^{|\mathcal{P}_M|} \frac{\mathcal{P}_{M,i}}{\mathcal{E}_{M,i}}\right)^{-1}\right)_{\text{dB}} + \left(\frac{W_I(d_{\text{free}})}{4k_c}\right)_{\text{dB}} \right] / 10. \end{aligned} \quad (29)$$

By comparing (29) and (28), we clearly see that the i.i.d. and spatially-correlated BER curves are parallel, which demonstrates that the spatial correlation does not effect the diversity order. Moreover, we see that there is an SNR shift between the curves. To further investigate this SNR shift, we require the following result from [13]:

⁵Note that this result agrees with the i.i.d. Chernoff bound we have derived differently in [4].

Lemma 1: If \mathbf{X} is an $m \times m$ Hermitian positive definite matrix, then

$$\frac{\text{tr}_m(\text{diag}(\mathbf{X}))}{\text{tr}_m(\lambda(\mathbf{X}))} \geq \frac{\text{tr}_{m-1}(\text{diag}(\mathbf{X}))}{\text{tr}_{m-1}(\lambda(\mathbf{X}))} \geq \dots \geq \frac{\text{tr}_1(\text{diag}(\mathbf{X}))}{\text{tr}_1(\lambda(\mathbf{X}))} = 1. \quad (30)$$

For convenience, we consider the case where $N_r = N_t = n$, for which K_R and K_S reduce to

$$K_R = \frac{n \det(\mathbf{R})}{\text{tr}_{n-1}(\lambda(\mathbf{R}))} \quad (31)$$

and

$$K_S = \left(\frac{1}{n \det(\mathbf{S})} \sum_{i=1}^{|\mathcal{P}_M|} \frac{\mathcal{P}_{M,i}}{\mathcal{E}_{M,i}} \sum_{k=1}^n \det(\mathbf{S}^{kk}) \right)^{-1} \\ = \frac{n \det(\mathbf{S})}{\text{tr}_{n-1}(\mathbf{S})} \left(\sum_{i=1}^{|\mathcal{P}_M|} \frac{\mathcal{P}_{M,i}}{\mathcal{E}_{M,i}} \right)^{-1}. \quad (32)$$

Note that the e.s.f. definition (17) was used in obtaining (32). Next, we substitute (31) and (32) into (28) and directly compare the resulting expression with (29). We find that for a given BER, the SNR difference between the i.i.d. and spatially-correlated curves is

$$\Delta_{dB} = \gamma_{\text{iid}} - \gamma_{\text{corr}} \\ = \left(\frac{n \det(\mathbf{R})}{\text{tr}_{n-1}(\lambda(\mathbf{R}))} \right)_{\text{dB}} + \left(\frac{n \det(\mathbf{S})}{\text{tr}_{n-1}(\lambda(\mathbf{S}))} \right)_{\text{dB}}. \quad (33)$$

To determine the sign of Δ_{dB} , we consider the receive correlation term, and write

$$\left(\frac{n \det(\mathbf{R})}{\text{tr}_{n-1}(\lambda(\mathbf{R}))} \right)_{\text{dB}} = \left(n \frac{\text{tr}_n(\lambda(\mathbf{R}))}{\text{tr}_{n-1}(\lambda(\mathbf{R}))} \right)_{\text{dB}} \\ \leq \left(n \frac{\text{tr}_n(\text{diag}(\mathbf{R}))}{\text{tr}_{n-1}(\text{diag}(\mathbf{R}))} \right)_{\text{dB}} \\ = 0 \quad (34)$$

where the second line followed from Lemma 1, and the last line followed by noting that the normalized correlation matrices have unity diagonal entries. Note that equality in (34) is achieved only if $\mathbf{R} = \mathbf{I}_{N_r}$. This result shows that for $n \times n$ ZF-BICM systems, the presence of transmit and receive correlation yields a net SNR loss at high SNR which is quantified by (33). This loss is a function of the antenna configuration and the eigenvalues of the spatial correlation matrices, and is independent of the coding and modulation scheme employed.

IV. NUMERICAL RESULTS

For our numerical results we generate the correlation matrices using the practical channel model considered in [16]. The model assumes that there are uniform linear arrays (ULA) at both the transmitter and receiver. Let us denote the relative antenna spacing between adjacent antennas (measured in number of wavelengths) as d_r at the receiver and d_t at the transmitter. Also, define $\theta_r, \theta_t, \sigma_r^2$ and σ_t^2 as the mean angle of arrival (AoA), mean angle of departure (AoD), receive angle spread and transmit angle spread respectively, and let $\underline{\theta}_r = \theta_r + \hat{\theta}_r$

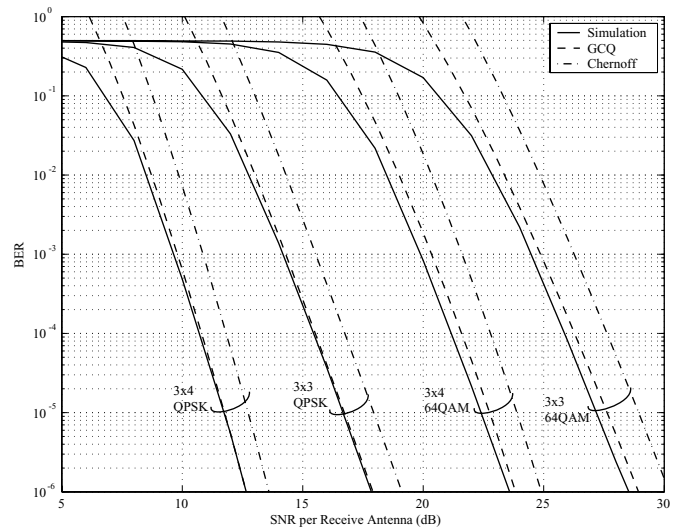


Fig. 2. Simulated and analytical BER results for a MIMO-BICM system with a ZF receiver, employing a 1/2 rate code. Results are shown for various antenna configurations and modulation schemes. The spatial correlation parameters are $\theta_r = \frac{\pi}{2}$, $\theta_t = \frac{\pi}{2}$, $\sigma_r^2 = \frac{\pi}{16}$, $\sigma_t^2 = \frac{\pi}{32}$ and $d_t = d_r = \frac{1}{2}$.

and $\underline{\theta}_t = \theta_t + \hat{\theta}_t$ denote the actual AoA and AoD, with $\hat{\theta}_r \sim \mathcal{N}(0, \sigma_r^2)$ and $\hat{\theta}_t \sim \mathcal{N}(0, \sigma_t^2)$. With these definitions, the $(p, q)^{\text{th}}$ entry of \mathbf{R} and \mathbf{S} is given by

$$\mathbf{R}_{p,q} = e^{-j2\pi(q-p)d_r \cos(\theta_r)} e^{-\frac{1}{2}(2\pi(q-p)d_r \sin(\theta_r)\sigma_r)^2} \\ \mathbf{S}_{p,q} = e^{-j2\pi(p-q)d_t \cos(\theta_t)} e^{-\frac{1}{2}(2\pi(p-q)d_t \sin(\theta_t)\sigma_t)^2}.$$

As mentioned in [16], the correlation function is essentially Gaussian with a spread inversely proportional to the product of the antenna spacing and cluster angle spread. This agrees with the intuition that smaller antenna spacing or angle spreads will generally lead to higher levels of spatial correlation. For all results in this section we assume $d_r = d_t = \frac{1}{2}$ and $\theta_r = \theta_t = \frac{\pi}{2}$.

Fig. 2 compares the analytical BER expressions with simulation results for 3×3 and 3×4 systems, with QPSK and 64QAM modulation. We consider the optimal 64-state 1/2 rate binary convolutional code with generator polynomials $(133, 171)_8$ (octal), and $d_{\text{free}} = 10$. The correlation parameters are $\sigma_r^2 = \frac{\pi}{16}$ and $\sigma_t^2 = \frac{\pi}{32}$. The dashed curve is based on the C-PEP expression (19), and is clearly tight for low to moderate BERs. The BER curves based on the C-PEP Chernoff bound (22) are also shown, and we see that the diversity order predicted from this bound matches the simulations.

Fig. 3 gives the tight BER curves based on the C-PEP (19), for 2×2 and 4×4 systems with QPSK modulation, and the 1/2 rate code above. Curves are presented for spatially-correlated channels with $\sigma_t^2 = \frac{\pi}{8}$ and different receive angle spreads, yielding different correlation scenarios. For reference, i.i.d. Rayleigh curves are also shown. As predicted from (28), we see that the diversity order is unaffected by the spatial correlation. Moreover, we see that both the 2×2 and 4×4 systems suffer an SNR loss due to the spatial correlation (with respect to i.i.d. Rayleigh), which increases as the receive angle spread is reduced. It can be easily verified that the SNR gaps in Fig. 3 agree almost exactly with the predictions from (33),

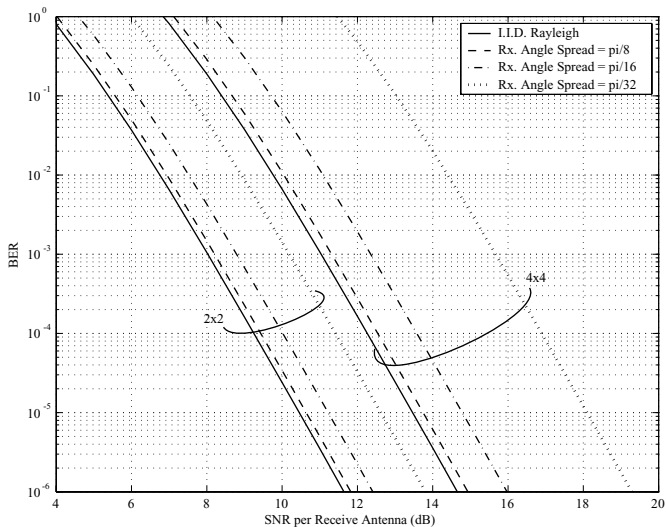


Fig. 3. Tight analytical BER curves for 2×2 and 4×4 MIMO-BICM systems with a ZF receiver, employing QPSK modulation. Results are shown for i.i.d. Rayleigh channels, as well as spatially-correlated channels with parameters $\theta_r = \frac{\pi}{2}$, $\theta_t = \frac{\pi}{2}$, $\sigma_r^2 = \frac{\pi}{8}$, $d_t = d_r = \frac{1}{2}$, and various σ_t^2 .

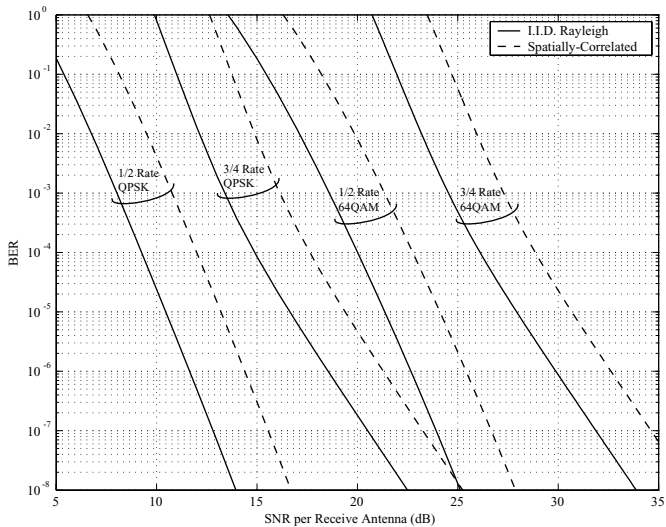


Fig. 4. Tight analytical BER curves for a 2×2 MIMO-BICM system with a ZF receiver, and with various coding/modulation combinations. Results are shown for i.i.d. Rayleigh channels, and for spatially-correlated channels with parameters $\theta_r = \frac{\pi}{2}$, $\theta_t = \frac{\pi}{2}$, $\sigma_r^2 = \frac{\pi}{16}$, $\sigma_t^2 = \frac{\pi}{32}$ and $d_t = d_r = \frac{1}{2}$.

which were derived based on the (looser) Chernoff bound. We mention that, for the 2×2 case in Fig. 3, (33) reduces to

$$\begin{aligned} \Delta_{\text{dB}} &= 10 \log_{10} \det(\mathbf{R}) + 10 \log_{10} \det(\mathbf{S}) \\ &= 10 \log_{10} \left(1 - e^{-\pi^2 \sigma_r^2}\right) + 10 \log_{10} \left(1 - e^{-\pi^2 \sigma_t^2}\right) \end{aligned} \quad (35)$$

which explicitly shows the SNR gap varying inversely to the angle spread.

Fig. 4 gives the tight BER curves based on the C-PEP (19), for a 2×2 system with QPSK and 64QAM modulation, and for 1/2 and 3/4 rate codes. The 3/4 rate code has $d_{\text{free}} = 5$ and is obtained by puncturing the 1/2 rate code above, with puncturing pattern given in [17]. Curves are presented for

correlated channels with parameters $\sigma_r^2 = \frac{\pi}{16}$ and $\sigma_t^2 = \frac{\pi}{32}$. I.i.d. Rayleigh curves are also given for reference. As predicted from (28), we clearly see that the diversity order is higher for the 1/2 rate code than the 3/4 rate code due to the larger free distance. Moreover, for all coding and modulation combinations, we see that the spatial correlation curves incur a constant SNR loss of approximately 2.7 dB with respect to the i.i.d. Rayleigh curves, which match almost exactly with the predictions from (33).

V. CONCLUSION

We presented tight analytical expressions for the coded BER of ZF-BICM in spatially-correlated MIMO channels. The analysis did not rely on standard BICM expurgation techniques and resulted in simple efficient expressions for the error probability. We obtained the diversity order, and demonstrated that it is unaffected by spatial correlation. We showed that spatial correlation induced an SNR loss with respect to i.i.d. channels. This loss was quantified, and was shown to be a function of the antenna configuration and the eigenvalues of the spatial correlation matrices, and was independent of the coding and modulation parameters.

REFERENCES

- [1] G. Caire, G. Taricco, and E. Biglieri, "Bit-interleaved coded modulation," *IEEE Trans. Inform. Theory*, vol. 44, no. 3, pp. 927–946, May 1998.
- [2] S. H. Müller-Weinfurter, "Coding approaches for multiple antenna transmission in fast fading and OFDM," *IEEE Trans. Signal Processing*, vol. 50, no. 10, pp. 2442–2450, Oct. 2002.
- [3] M. R. G. Butler and I. B. Collings, "A zero-forcing approximate log-likelihood receiver for MIMO bit-interleaved coded modulation," *IEEE Commun. Lett.*, vol. 8, no. 2, pp. 105–107, Feb. 2004.
- [4] M. R. McKay and I. B. Collings, "Capacity and performance of MIMO-BICM with zero-forcing receivers," *IEEE Trans. Commun.*, vol. 53, no. 1, pp. 74–83, Jan. 2005.
- [5] A. J. Viterbi and J. K. Omura, *Principles of Digital Communication and Coding*. New York: McGraw-Hill, 1979.
- [6] J. G. Proakis, *Digital Communications*, 4th ed. New York: McGraw-Hill, 2001.
- [7] M. Abramowitz and I. A. Stegun, *Handbook of Mathematical Functions with Formulas, Graphs, and Mathematical Tables*, 9th ed. New York: Dover Publications, 1970.
- [8] E. Biglieri, G. Caire, G. Taricco, and J. Ventura-Traveset, "Simple method for evaluating error probabilities," *Electronic Letters*, vol. 32, no. 3, pp. 191–192, Feb. 1996.
- [9] R. Durrett, *Probability: Theory and Examples*, 2nd ed. Duxbury Press, 1996.
- [10] A. Martinez, A. G. I. Fabregas, and G. Caire, "Error probability analysis of bit-interleaved coded modulation," *IEEE Trans. Inform. Theory*, submitted for publication.
- [11] O. Lieberman, "A Laplace approximation to the moments of a ratio of quadratic forms," *Biometrika*, vol. 81, no. 4, pp. 681–690, 1994.
- [12] M. Kiessling and J. Speidel, "Asymptotically tight bound on SER of MIMO zero-forcing receivers with correlated fading," in *IEEE Int. Symp. on Information Theory (ISIT)*, 2004, p. 501.
- [13] A. W. Marshall and I. Olkin, *Inequalities: Theory of Majorization and Its Applications*, 1st ed. New York: Academic Press, 1979.
- [14] R. A. Horn and C. R. Johnson, *Matrix Analysis*, 4th ed. New York: University of Cambridge Press, 1990.
- [15] R. Gallager, *Information Theory and Reliable Communication*. John Wiley and Sons, 1968.
- [16] H. Bölcskei, M. Borgmann, and A. J. Paulraj, "Impact of the propagation environment on the performance of space-frequency coded MIMO-OFDM," *IEEE J. Select. Areas Commun.*, vol. 21, no. 3, pp. 427–439, Apr 2003.
- [17] IEEE 802.11, "Supplement to IEEE standard for telecommunications and information exchange between systems - LAN and MAN specific requirements," IEEE Std 802.11a-1999, September 1999.



Matthew R. McKay (S'03) is from Meningie, Australia, and was born in 1979. He received the combined B.E. degree in Electrical Engineering and B.IT. degree in Computer Science from the Queensland University of Technology, Brisbane, in 2002, and received the University Medal upon graduating. He is currently working toward the Ph.D. degree in Electrical Engineering at The University of Sydney. His research is supported by the Information and Communication Technologies (ICT) Centre at Australia's Commonwealth Scientific & Industrial

Research Organisation (CSIRO) where he is a recipient of a Postgraduate scholarship.

His current research interests include MIMO-OFDM, bit-interleaved coded modulation, information theory, adaptive signal processing, and multivariate statistical theory.



Iain B. Collings (S'92-M'95-SM'02) was born in Melbourne, Australia, in 1970. He received the B.E. degree in Electrical and Electronic Engineering from the University of Melbourne in 1992, and the Ph.D. degree in Systems Engineering from the Australian National University in 1995.

Currently he is a Science Leader in the Wireless Technologies Laboratory at the CSIRO ICT Centre, Australia. Prior to this he was an Associate Professor at the University of Sydney (1999-2005); a Lecturer at the University of Melbourne (1996-1999); and a

Research Fellow in the Australian Cooperative Research Centre for Sensor Signal and Information Processing (1995). His current research interests include mobile digital communications and broadband digital subscriber line communications. More specifically, synchronization, channel estimation, equalization, and multi-carrier modulation, for time-varying and frequency-selective channels.

Dr Collings currently serves as an Editor for the IEEE Transactions on Wireless Communications, and as a Guest Editor for the EURASIP Journal on Advanced Signal Processing. He has also served as the Vice Chair of the Technical Program Committee for IEEE Vehicular Technology Conf. (Spring) 2006, as well as serving on a number of other TPCs and organizing committees of IEEE conferences. He is also a founding organizer of the Australian Communication Theory Workshops 2000-06.